Lowering of threshold conditions for nonlinear effects in a microsphere

D. Braunstein, A. M. Khazanov, G. A. Koganov, and R. Shuker
Physics Department, Ben Gurion University of the Negev, Beer Sheva 84105, Israel
(Received 5 April 1995; revised manuscript received 17 January 1996)

An explicit relationship between the Lorenz-Mie resonances and nonlinear optics of a microsphere has been found. We have constructed an approximate analytic method which allows an adequate assessment of the threshold for stimulated Raman scattering in microspheres. Systematic investigation of the characteristic equation, using approximate analytic expressions, reveals that not all modes have the same quality. Some resonances with very high quality correspond to a physical situation in which the spherical waves can be envisioned as whispering-gallery light waves that are totally internally reflected by the sphere boundary, without suffering almost any loss.

PACS number(s): 42.50.Dv

I. INTRODUCTION

A dielectric microsphere possesses natural modes of light oscillation at characteristic frequencies corresponding to specific size to wavelength ratios. These structure resonances, sometimes called ''morphology dependent resonances,'' are known to cause extremely large field intensities within the spherical cavity, very narrow modes, high density of electromagnetic (EM) modes, and hence have extremely large theoretical quality factors $Q \approx 10^{20}$ [1,2]. These characteristics impart very low threshold conditions for nonlinear processes [3]. Transparent microspheres act as high-Q resonators with the feedback provided by the whispering light waves.

A variety of interesting nonlinear phenomena in microdroplets have been reported: Cavity QED effects [4], spontaneous emission from droplets showing intense spectral peaks superimposed on the normal bulk emission [5] as well as modified fluorescence lifetimes [6], enhanced lasing [7], and Raman gains [8] . Third order nonlinear optical effects, normally seen in bulk liquids only under intense nanosecond pulse excitation, were reported to be observed at low power cw excitation in microdroplets [9,10]. Theoretical work on stimulated Brillouin scattering has also been reported [11,12]. This extremely low threshold can be attributed to interacting waves simultaneously resonant with high-Q droplet modes and to the presence of significant QED enhancement of nonlinear gain.

Sharp resonances have been studied both analytically and numerically in a number of publications [3,13]. However, most of the publications, as rigorous as they are, deal with calculations of passive resonances and have been too qualitative with regard to nonlinear optics. Moreover, as we shall see, there are more limitations on threshold enhancement than just the narrowness of the resonances. Because of that we try here to clarify the relationship between the passive resonances and nonlinear optics. We suggest a set of theoretical approximations that allow one to simply and reliably evaluate the threshold condition for nonlinear phenomena. At the same time, the theory presented is quite general. Though our theory is quite general, we illustrate it only on stimulated Raman scattering (SRS).

We start from some basics of Lorenz-Mie theory. The sphere can be treated as a body bounded by a closed surface within which a system of standing waves can be set up. The electric and magnetic fields inside a homogeneous, isotropic, and source-free dielectric microsphere of radius a are represented in terms of vector spherical harmonic wave functions. For a plane wave excitation, linearly polarized in the x direction and propagating along the z axis, the expression for the electric field takes the form

$$\mathbf{E}(\mathbf{r},t) = e^{-i\omega t} \sum_{n=1}^{\infty} E_0 i^n \frac{2n+1}{n(n+1)} (c_n \mathbf{M}_{o,1,n}^{(1)} - i d_n \mathbf{N}_{e,1,n}^{(1)}), \tag{1}$$

where $\mathbf{M}$ and $\mathbf{N}$ are the vector spherical harmonic functions of the first kind [14]. c_n represents the internal field expansion coefficients (we discuss here only TE modes). Imposing the relevant boundary conditions yields the following expression of the internal electric field expansion coefficients:

$$c_n = \frac{j_n(\rho)[\rho h_n^{(1)}(\rho)]' - h_n^{(1)}(\rho)[\rho j_n(\rho)]'}{j_n(m\rho)[\rho h_n^{(1)}(\rho)]' - h_n^{(1)}(\rho)[m\rho j_n(m\rho)]'}. \tag{2}$$

Here m stands for the relative refractive index, ρ is the size parameter defined by $\rho = k_2 a$, where k_2 is the wave number in the surrounding medium, and the derivatives are with respect to the function argument. $j_n(\rho)$ and $h_n^{(1)}(\rho)$ are the spherical Bessel function and spherical Hankel functions of the first and third kind, respectively. Amplitude enhancement factors correspond to the roots of the characteristic equation. These are just the roots of the denominator in Eq. (2), i.e., when the following transcendental equation is obeyed:

$$\frac{[m\rho j_n(m\rho)]'}{j_n(m\rho)} = \frac{[\rho h_n^{(1)}(\rho)]'}{h_n^{(1)}(\rho)} \text{ TE modes.} \tag{3}$$

Equation (3) contains all the necessary physical information regarding the position, width, spacing, and strength of the resonances. The characteristic equation is solved by a set of discrete roots labeled $\rho_{n,s}$ that correspond to the number s solution for a given principal mode number n. These roots (size parameter) are complex, and define eigenfrequencies of virtual modes which represent radiative solutions of the Maxwell equations. The modes are termed virtual since their size parameter is a complex number. The real and imaginary parts of the size parameter define resonance positions and

width, respectively, and hence dictate the radiative lifetime of the mode. Natural resonant frequencies associated with the modes are given by [14]

$$\omega_{n,s}=\frac{1}{\varepsilon}\sqrt{\frac{\varepsilon c^2\rho_{n,s}^2}{a^2}-4\pi^2\sigma^2}-i\frac{2\pi\sigma}{\varepsilon}, \tag{4}$$

where ε is the dielectric constant of the surrounding medium and σ represents its conductivity. We have assumed a nonmagnetic medium ($\mu=1$). Complex roots, $\rho_{n,s}$, of the characteristic equation account for the leakage losses, which may be present even if the material conductivity σ is zero. The reason for this behavior is that the characteristic equation is explicitly complex even if the relative index of refraction is purely real, thus the size parameters $\rho_{n,s}$ are also complex. They actually represent the evanescentlike waves. For actual frequency excitation, the c_n coefficient cannot have an infinite amplitude. However, a sharp finite amplitude is possible. Resonances occur when the real size parameter approaches the complex roots of the characteristic equation.

There are mainly two mechanisms responsible for energy losses inside the spherical cavity.

(1) Ohmic losses by heating of the medium. These are represented explicitly by the conductivity term σ.

(2) Inherent energy leakage (the field escaping outside the sphere via the evanescent waves). This mechanism is represented mathematically by the imaginary part of the size parameter. It is the mechanism responsible for the very high quality of some cavity modes, since once matter is present we almost cannot control the Ohmic losses.

As will be seen, the imaginary part of the eigenfrequency depends on the indices n and s. Under certain conditions, which we discuss in detail in this article, the damping can be made vanishingly small (the characteristic equation has almost pure real roots). The reduction of the linewidth results in the enhancement of the mode lifetime, hence investigation of various nonlinear phenomena in microspheres will be especially interesting. The enhancement in the mode quality corresponds to a physical situation, in which the spherical standing wave behaves like a ray of light, which is totally reflected by the internal surface of the sphere without suffering almost any losses (total internal reflection). It is interesting to note that microsphere resonances are narrow Lorentzians to first approximation, and are in fact exponentially narrower.

In the following section, we investigate the influence of different asymptotic behaviors of the spherical Bessel functions on the mode width.

II. ASYMPTOTIC BEHAVIOR OF SPHERICAL BESSEL FUNCTIONS AND THE QUALITY OF MODES

In this section we examine the conditions under which the linewidth, and hence the damping constant, of the spherical wave become minimal. The required information is contained in the characteristic equation which completely determines the frequencies and the width of the resonances. In order to acquire the desired information we solve the characteristic equation for the roots $\rho_{n,s}$. This characteristic equation has no vector features and thus can be treated as a purely scalar problem. Since this equation is transcendental, one must either use a numerical approach or search for an appropriate approximation for the Bessel functions $j_n(kr)$ and $h_n^1(kr)$. The numerical approach has already been undertaken in many works (see, for example [3]). Although these solutions have quite a high precision and have been developed for Bessel functions of high order, they unfortunately do not contribute to the physical understanding of the enhancement of the mode quality. Moreover, the numerical approach does not provide analytic expressions for the damping constants which are of crucial importance for the quantitative assessment of the threshold parameters of various nonlinear phenomena. We therefore consider the following various approximations to the Bessel functions. A more accurate treatment can be found in the work of Lam, Leung, and Young [13]. Our approach, though much simpler, covers all the meaningful asymptotic regions of the Bessel functions not treated earlier by this group. What follows is then an asymptotic treatment of spherical Bessel function. The Airy functions approximation was found to be the most fruitful. It reads [15]

$$h_n^{(1)}=\sqrt{\frac{\pi}{6\rho}}w\exp\left\{i\left[\nu\left(w-\frac{w^3}{3}-\arctan w\right)+\frac{\pi}{6}\right]\right\}\times H_{1/3}^{(1)}\left(\frac{\nu w^3}{3}\right)+o\left(\frac{1}{\nu}\right), \tag{5}$$

where $H_{1/3}$ is the cylindrical Hankel function of the first kind and of order $\frac{1}{3}$, and $\nu=n+1/2$. The error $o(1/\nu)$ does not exceed the value $24\sqrt{2}/\nu$, and thus the approximation is expected to be better for large indices ν. The parameter w, given by $w=\sqrt{(\rho/\nu)^2-1}$, is the characteristic parameter of the different regions. It is a measure of the deviation of the argument ρ from the point $\rho=\nu$.

A. The trigonometric region (optical geometric limit)

Here we assume the parameter w to be much larger than unity, which means that the argument of the Bessel functions is much greater than its index (the trigonometric approximation [15]). As a consequence we may write

$$H_{1/3}^{(1)}(x)\approx\sqrt{\frac{2}{\pi x}}\exp\left[i\left(x-\frac{\pi}{6}-\frac{\pi}{4}\right)\right], \tag{6}$$

where

$$\arctan w\approx\frac{\pi}{2}. \tag{7}$$

Here we have used the trigonometric approximation for the Hankel function. Making these approximations, one easily obtains for the spherical Hankel function

$$h_n^{(1)}(\rho)\approx(-i)^{(n+1)}\frac{e^{i\rho}}{\rho}. \tag{8}$$

If the argument ρ for the outgoing external wave corresponds to the trigonometric region, i.e., it obeys the conditions under which the trigonometric approximation is valid, then the internal wave is even more so, because the argument of the internal wave is multiplied by $m>1$. Substitution of the

trigonometric approximation in the characteristic equation (3) for both waves yields the following simple characteristic equation:

$$\frac{i}{m}\cos\gamma+\sin\gamma=0, \tag{9}$$

where γ is defined by

$$\gamma=m\rho+\frac{\pi}{2}(n+1). \tag{10}$$

For a real index of refraction, we obtain for the resonance positions and width, respectively,

$$\mathrm{Re}(\rho_{n,s})=\frac{s\pi}{m}+\frac{\pi}{2m}(n+1), \tag{11}$$

$$\Gamma=-2\mathrm{Im}(\rho_{n,s})=\frac{1}{m}\ln\frac{m+1}{m-1}. \tag{12}$$

Inspection of the last two expressions yields the following conclusions.

(1) All the resonances have the same width.

(2) The distance between resonances is constant.

(3) These resonances are much wider than those observed experimentally [16].

To conclude this subsection we observe that the resonances obtained by replacing Bessel functions by their trigonometric approximation do not reflect the physical situation observed in experiments, so we should discard them as physically irrelevant. In fact these resonances ''reside'' far away from the sphere surface.

B. Stationary phase region and refractive index renormalization

In this region we assume the parameter w to be a number of the order unity or less, but not too close to the point $\rho=\nu$ (our approximation breaks down when the argument ρ is in the neighborhood of the radius $\nu^{1/3}$ right to the point $\rho=\nu$). If, in addition, we assume that the cylindrical Hankel function can be replaced by its trigonometric approximation, which is obviously justified, provided that the order ν is large enough, we obtain the well known stationary phase approximation to the spherical Bessel functions

$$h_n^{(1)}(\rho)=\frac{1}{\sqrt{\rho\nu w}}\exp i\left[\nu(w-\arctan w)-\frac{\pi}{4}\right], \tag{13}$$

or in a more familiar form, in terms of the angle β defined by $\cos\beta=\nu/\rho$,

$$h_n^{(1)}(\rho)=\frac{1}{\sqrt{\rho\nu\tan\beta}}\exp i\left[\nu(\tan\beta-\beta)-\frac{\pi}{4}\right]. \tag{14}$$

We assume that the argument of the internal wave belongs to the trigonometric approximation and substitute the corresponding asymptotic expressions in the characteristic equation, (3). Doing so we obtain

$$\frac{1}{m}\left[\left(\frac{1}{\rho}+\frac{A'}{A}\right)+i\phi'\right]\cos\gamma+\sin\gamma=0, \tag{15}$$

where $A(\rho)$ and $\phi(\rho)$ are the amplitude and phase of the stationary phase region. Let us compare Eq. (15) and its analog Eq. (9). The term in parentheses, $1/\rho+A'/A\approx-1/2\nu$, being a real quantity, describes a small correction (of order ν^{-1}) to the resonance position. The imaginary term describes the width of resonance. We remark here that we are not interested in exact calculation of resonance positions, but rather we wish to obtain an order of magnitude for the width in different regions. Hence we would allow ourselves to neglect the small real term with respect to the imaginary term in Eq. (15). The width of the resonance in the stationary phase region retains its form Eq. (12), provided that the refractive index was renormalized:

$$\Gamma=\frac{1}{m_{\mathrm{ren}}}\ln\frac{m_{\mathrm{ren}}+1}{m_{\mathrm{ren}}-1}, \tag{16}$$

where

$$m_{\mathrm{ren}}=m/\sin\beta. \tag{17}$$

The last expression indicates a broad margin for narrowing the width, due to the presence of the factor $1/\sin\beta$ in m_{ren} ($m_{\mathrm{ren}}>m$), since β can be a small number. Renormalization of the refractive index indicates morphological focusing (the sphere can be envisioned as a microlens) and thus it is expected to lead to a more pronounced self-focusing nonlinear effect. Furthermore, in the stationary phase region the resonance positions and widths are size parameter dependent, which is a more realistic description of the resonances observed experimentally. In addition, the width appears to decrease significantly compared to that obtained in the trigonometric region.

C. No oscillation region

The damping constant can still be drastically decreased. Let ρ correspond to the region characterized by purely imaginary w parameter (the argument is smaller than the index). We call this region the ''no oscillation region'' because Bessel functions do oscillate there. Our main approximation formula (5) still holds, but w is purely imaginary, as mentioned before. It is convenient to use here the real quantity p defined as $p=-iw$. The spherical Bessel function in the no oscillation region takes the form

$$h_n^{(1)}(\rho)\approx-i\frac{1}{\sqrt{\nu\rho p}}e^{\nu(\arctan hp-p)}. \tag{18}$$

While deriving the last expression we have neglected a similar real term, but with an opposite exponential dependence. Let us return now to the characteristic equation and substitute Eq. (18) for the external wave. Since the argument of the internal wave is $m\rho$, it will be reasonable to assume that it will be adequately described by the stationary phase approximation. However, the characteristic equation obtained by doing so turns out to predict resonance positions that systematically deviate from the exact positions calculated numerically from the exact characteristic equation. Thus in

order to improve the accuracy of our approximated characteristic equation we have included a term of the order of ν^{-1} in the expression for the stationary phase approximation, as follows:

$$j_n(y)=\frac{1}{\sqrt{\nu w_1 y}}\left(\cos\phi_1+\frac{\sin\phi_1}{8\nu w_1}\right), \tag{19}$$

where

$$y=m\rho \tag{20}$$

and

$$w_1=\sqrt{\frac{y^2}{\nu^2}-1}. \tag{21}$$

Substituting the last expression together with Eq. (18) in the characteristic equation one obtains the result

$$\sin\phi_1\left(\frac{\beta}{8\nu w_1}+\nu w_1\right)=-\cos\phi_1\left(\beta+\frac{3}{8}\right), \tag{22}$$

where

$$\beta=\frac{1}{2p^2}-\nu p-1. \tag{23}$$

The notable property of the last characteristic equation is that it is purely real, and thus does not describe damping at all. Physically, it means that the spherical mode does not experience any decay, unless we take into account active losses in the medium. Certainly, it corresponds to a very high quality of the cavity mode, which is restricted only by the conductivity of the dielectric sphere. In fact, the laser light under such circumstances is trapped within the sphere. However, the last equation was obtained after a series of approximations, during which the exact knowledge regarding the width was lost. Nevertheless, there is nothing in the last statement to undermine its importance. As we will see immediately, this equation nicely predicts resonance positions. In order to get a reliable expression for the linewidth we have followed Lam *et al.* (see [13]), by going to the complex k plane and seeking an approximate expression for the internal field expansion coefficient, suitable to the situation under consideration, i.e., to the case where the external wave corresponds to the no oscillation region, while the internal wave is described in terms of the stationary phase approximation. The resulting expression for the linewidth turns out to be very accurate and reliable, provided that we know to calculate resonance positions accurately enough. For a TE resonance the expression reads (in units of the size parameter ρ)

$$\Gamma_{\mathrm{TE}}=\frac{2}{(m^2-1)x_0^2 y_n^2(x_0)}. \tag{24}$$

Here Γ is the width at half maximum, x_0 is the real part of the size parameter, and y_n is the spherical Neumann function. The singularity in the last expression has a physical significance. As the relative index of refraction approaches unity the sphere ''disappears'' and thus resonances are not expected, so that Γ ought to go to infinity. Inspection of Eq. (24) reveals that the linewidth is expected to be an exponentially decreasing function of its order ν, as can be readily seen by considering the asymptotic behavior of the spherical Neumann function appearing in the denominator of Eq. (24).

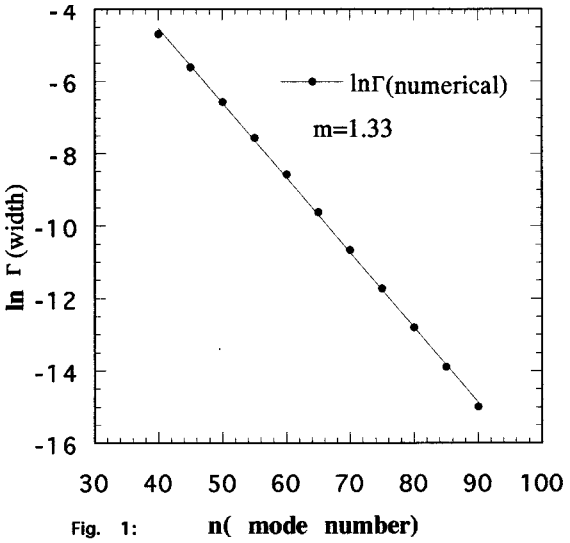

FIG. 1. Logarithm of width as a function of the principal mode number. We can see exponentially decreasing width.

In conclusion, the resonances discussed in this subsection are of a very high quality (small width) that might be almost entirely determined by the finite conductivity of the sphere. The reason for this behavior is that energy losses originating in the geometry of the problem will become smaller as the mode number increases, until eventually they would be ignorable relative to Ohmic losses. These modes are called whispering modes and in fact their path degenerates into the perimeter.

D. Comparison with numerical results

In this subsection we compare our predictions regarding resonance positions and width based on numerical solution of our approximated Eqs. (22) and (24), with exact numerical results. Exact resonance positions and width were calculated by solving numerically the exact characteristic equation, Eq. (3). Only first order resonances were considered for principal mode numbers ranging from $n=40$ to $n=90$. Figure 1 shows the logarithm of the exact width versus the principal mode number, from which we see that the width is *indeed* an exponentially decreasing function of the mode number. Figures 2 and 3 compare resonance positions and linewidth, normalized to the exact numerical values, obtained from our results and those of Lam *et al.* (see [13]), as a function of the mode number. The comparison yields the following.

(1) Relative errors are of the order of tenths of a percent, for resonance positions, and of about 4% for the width.

(2) Linewidths calculated by substitution of exact numerical resonance positions in the approximated expression are in good agreement with those calculated numerically. This supports the reliability of that expression. In other words, the analytic expression for linewidth is an excellent approximation, provided that accurate resonance positions are substituted.

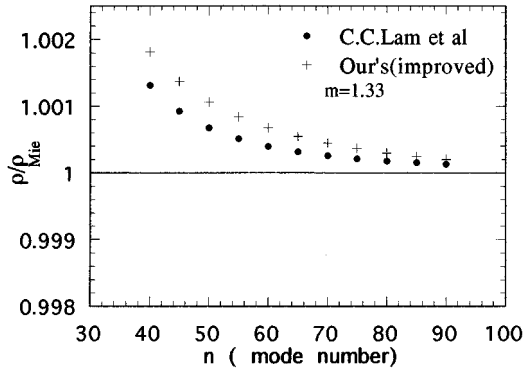

FIG. 2. Approximate resonance locations, normalized to exact values, ρ_{Mie}, as obtained by us (crosses) and Lam *et al.* (circles). The index of refraction is 1.33.

(3) Relative errors decrease for large mode numbers, as expected from the type of approximation we have used.

To conclude our numerical comparison, we can say with confidence that our approximated characteristic equation and the expression for the linewidth correctly predict resonance positions and width, especially for waves with large angular momentum. The apparent small advantage over the procedure proposed by Lam *et al.* is expected to diminish with increasing mode number. Our proposed procedure necessitates the solution of a very simple characteristic equation and can be used as a reliable and fast alternative to the exact numerical solution, or at least as a fine starting point for more accurate numerical computation, employing Newton's method. The investigation of mode quality in this section covers all the meaningful regions of mode behavior, and thus is more general than the work done to date.

III. STIMULATED RAMAN SCATTERING IN MICROSPHERES

We discuss now stimulated Raman scattering from microspheres, where our motivation is to get an analytic expression for the threshold intensity, required by this process. In order to achieve this task we need to establish a connection between the usual nonlinear SRS process and the microsphere formalism. We shall see that under certain conditions it is possible to get a substantial reduction of the threshold condition. The reduction of the threshold intensity can be attributed to the enhancement of the amplification constant, due to the creation of large fields, with the necessary feedback provided by the whispering waves on one hand, and to QED enhancement of nonlinear gain on the other hand [9]. The effect of QED enhancement of nonlinear gain will not be discussed here.

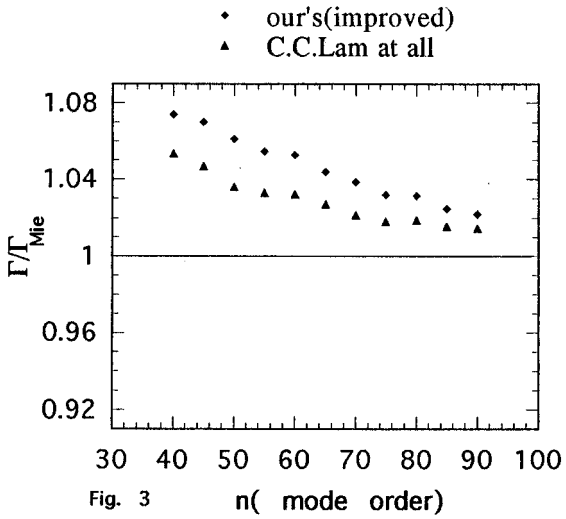

FIG. 3. Approximate widths, normalized to exact values, Γ_{Mie}, as obtained by us (diamonds) and Lam *et al.* (triangles). The index of refraction is 1.33.

A. Laser-Stokes coupling equations

In stimulated Raman scattering two waves of high intensity and of frequencies ω_l (referred to as the laser wave) and ω_s (referred to as the Stokes wave) are mixed together in the medium to produce an induced polarization, which in turn will act as a source for new coherent waves. The signal (at ω_s) is enhanced if $\omega_s=\omega_l-\Omega$, where Ω is the Raman active resonance in the medium (atomic transition frequency). For the sake of simplicity we assume here that no phase matching condition is obeyed, and hence no anti-Stokes waves and higher terms are present. In addition we assume that the input frequencies coincide with high-Q cavity modes. The coupling between the waves is governed by a set of two coupled wave equations (the coupling is brought by the nonlinear polarization terms)

$$\nabla\times\nabla\times\mathbf{E}_l+\frac{\epsilon_l}{c^2}\frac{\partial^2\mathbf{E}_l}{\partial t^2}=\frac{4\pi\omega_l^2}{c^2}\mathbf{P}_{Nl}^{(3)}(\omega_l)e^{-i\omega_l t},$$
$$\nabla\times\nabla\times\mathbf{E}_s+\frac{\epsilon_s}{c^2}\frac{\partial^2\mathbf{E}_s}{\partial t^2}=\frac{4\pi\omega_s^2}{c^2}\mathbf{P}_{Nl}^{(3)}(\omega_s)e^{-i\omega_s t}, \tag{25}$$

where $\mathbf{E}_i$ are the fields inside the sphere, $\mathbf{P}_{Nl}^{(3)}(\omega_i)$ are the Fourier components of the third order nonlinear polarization, and ϵ_i are the dielectric constants, at the corresponding frequencies. The problem now is to express the polarization as a function of the interacting waves, for the set of equations (25) to be closed. We derive these expressions by considering a classic model for the stimulated Raman process, adjusted to the spherical geometry. This results in the expression

$$\mathbf{P}_{Nl}^{(3)}(\omega_s)=6\chi_R^{(3)}(\omega_s)|A_l|^2A_s(\mathbf{e}_s\cdot\mathbf{e}_l)\mathbf{e}_l,$$
$$\mathbf{P}_{Nl}^{(3)}(\omega_l)=6\chi_R^{(3)}(\omega_l)|A_s|^2A_l(\mathbf{e}_l\cdot\mathbf{e}_s)\mathbf{e}_s, \tag{26}$$

where $\chi_R^{(3)}(\omega_i)$ is the third order nonlinear electric susceptibility, $\mathbf{e}_i(\mathbf{r})$ are the spatial parts of the fields, which correspond to a specific spherical mode, and the amplitudes A_i are slowly varying in time with respect to the optical oscillations and are related to the fields $\mathbf{E}_i$ through the relation

$$\mathbf{E}_i=A_i(t)e^{-i\omega_i t}\mathbf{e}_i(\mathbf{r}),\quad i=l,s. \tag{27}$$

A significant simplification of Eq. (25) can be obtained by considering the representation (27), taking into account that the spatial part must obey the wave equation, i.e.,

$$\nabla\times\nabla\times\mathbf{e}_i(\mathbf{r})=k_i^2\mathbf{e}_i(\mathbf{r}). \tag{28}$$

We make use of the slowly varying envelope approximation (SVEA) $|\partial^2 A/\partial t^2|\ll\omega|\partial A/\partial t|$, taking into account only the equations for the real part of the amplitudes ($\widetilde{A}_i$). This results in the relations

$$\frac{d\widetilde{A}_l}{dt}+\Gamma_l(\widetilde{A}_l-\widetilde{A}_l^{\mathrm{SS}})=\beta_l|A_s|^2(\widetilde{A}_l-\widetilde{A}_l^{\mathrm{SS}}), \tag{29}$$

$$\frac{d\widetilde{A}_s}{dt}+\Gamma_s\widetilde{A}_s=\beta_s|A_l|^2\widetilde{A}_s, \tag{30}$$

with the definitions

$$\Gamma_i=\Gamma_{\mathrm{abs}}+\frac{c}{am}\Gamma(\rho),\quad i=l,s \tag{31}$$

and

$$\beta_j=\frac{12\pi\omega_j\mathrm{Im}[\chi_R^{(3)}(\omega_j)]\langle|\mathbf{e}_k|^2\rangle}{\epsilon_j},\quad j,k=l,s,\quad j\neq k. \tag{32}$$

While deriving the last equations we have performed volume average (denoted by $\langle\rangle$) over the spatial part, and introduced the steady state amplitude $\widetilde{A}_l^{\mathrm{SS}}$. The damping constant Γ_i is decomposed into two parts, where Γ_{abs} accounts for the absorption part and the second term accounts for leakage losses and should be calculated from the Lorenz-Mie theory. $\Gamma(\rho)$ is the width of the resonance in units of the dimensionless size parameter and β_j are the gain constants multiplied by the volume average quantities. The quantities $\widetilde{A}_l^{\mathrm{SS}}$ (steady state amplitude) and Γ_i (damping constants) will be determined from the Lorenz-Mie theory in the next section. The set of Eqs. (29), (30) allows one to study the dynamics of coupling between the laser wave (pump wave) and the Stokes wave. This study is beyond the scope of the present paper, where we only examine threshold conditions.

B. Threshold evaluation

Besides the damping constants there are other quantities in the basic coupling equations (29), (30) which also originate in Lorenz-Mie theory. These quantities are the steady state amplitude $\widetilde{A}_l^{\mathrm{SS}}$ and the volume averages, which will participate in threshold evaluation, as we shall see immediately. The threshold condition follows from the stationary solutions of (29), (30), i.e.,

$$|A_l^{\mathrm{SS}}|^2\geqslant\frac{\Gamma_s}{\beta_s}, \tag{33}$$

which is just a mathematical statement saying that threshold is achieved when the total gain (gain coefficient times the intensity, $\beta_s\times|A_l^{\mathrm{SS}}|^2$) exceeds losses ($\Gamma_s$). We evaluate the threshold in the most interesting case, i.e., when the external waves are represented by the ''no oscillation region'' (i.e., their argument is such that it can be represented by the ''no oscillation approximation''), while the internal waves are represented by the stationary phase approximation. In order to evaluate the threshold, we should first establish a connection between the steady state amplitude $\widetilde{A}_l^{\mathrm{SS}}$ and the amplitude of the external wave exciting the sphere, E_0. First let us define the spherical functions $\mathbf{e}_i(\mathbf{r})$ as

$$\mathbf{e}_i(\mathbf{r})=i^n\frac{2n+1}{n(n+1)}\mathbf{M}_{\mathbf{0,1,n}}^{(1)} \tag{34}$$

and represent the field in the same manner as in Eq. (27), i.e.,

$$\mathbf{E}_i=A_i(t)e^{-i\omega_i t}\mathbf{e}_i(\mathbf{r}). \tag{35}$$

Comparing the last two expressions with Eq. (1), for the case of single mode, TE type excitation, we arrive at the relation between the Maxwell amplitude E_0 and the internal field expansion coefficient, which reads $A_l=E_0c_n$. Remembering the resonant nature of the field expansion coefficient, we arrive at the conclusion that the maximization of the coefficient corresponds to a resonant event and thus we can write, for the steady state amplitude, $A_l^{\mathrm{SS}}=E_0\max\{c_n\}$. The steady state amplitude is calculated by substituting the relevant approximation for spherical Bessel functions, and maximizing the expression. For our case the procedure is most simple, once we have the approximate form (Lorenzian line shape) of the c_n coefficient. The c_n coefficient can be written near a TE resonance as (see [13])

$$c_n=\frac{y_n(\rho_0)}{j_n(\rho_0)}\frac{\Gamma_{\mathrm{TE}}/2}{(\rho-\rho_0)+i\Gamma_{\mathrm{TE}}/2}, \tag{36}$$

where $j_n(\rho_0)$, $y_n(\rho_0)$ are the spherical Bessel and Neumann function, evaluated at resonance, respectively. At resonance we may let $\rho\to\rho_0$, obtaining for the steady state amplitude

$$A_l^{\mathrm{SS}}=2E_0e^{2\nu(\arctan hp_{0,l}-p_{0,l})}, \tag{37}$$

where the subscript 0 reminds us that the parameter p should be evaluated at resonance positions only, and the subscript l reminds us that the corresponding term originates in the laser wave. In deriving Eq. (37) we have replaced the spherical Bessel function by its asymptotic approximation. In order to evaluate the volume average quantities we need to solve the relevant integral. The angular part can be found in many textbooks [14]. For the evaluation of the spherical part see Ref. [17]. Solving the integral we get for the volume average of the amplitude squared (intensity)

$$\langle|\mathbf{e}_l|^2\rangle=\frac{3n_l}{2}\frac{m^2-1}{m^2j_n^2(m\rho_{0,l})}. \tag{38}$$

Here n_l is the number of the resonance of the laser wave. Before getting to threshold evaluation, let us make some preliminary remarks. In stimulated Brillouin scattering (SBS), there exists a limit on the frequency shift Ω [12]. This can possibly cause the scattered frequency ω_s *not* to coincide with a morphology dependent resonance and hence one deals with a single resonance case. This limit does not exist in stimulated Raman scattering. In addition, because of the large width of the gain curve it is reasonable to expect that

the scattered frequency will also coincide with a morphology dependent resonance, thus having a double resonance situation (both pump and Stokes waves coincide with high-Q cavity modes). Taking this into account and assigning additional indices l and s, identifying the origin of the relevant terms, we obtain after substitution of the expressions for the steady state amplitude, and the volume average in Eq. (33), for the threshold condition

$$\alpha_{l,s}E_0^2 \geqslant \left[\frac{mc\nu_s p_{0,s} e^{-2\nu_s[\operatorname{arctanh}(p_{0,s})-p_{0,s}]}}{a(m^2-1)^2\rho_{0,s}}\right] \times \left[\frac{e^{-4\nu_l[\operatorname{arctanh}(p_{0,l})-p_{0,l}]}}{3n_l j_n^2(m\rho_{0,l})}\right]. \tag{39}$$

In obtaining the last expression we have neglected absorption losses relative to leakage losses. We also introduced a new gain constant independent of the volume average, defined by

$$\beta_i = \alpha_i \langle |\mathbf{e}_k|^2 \rangle, \quad i \neq k. \tag{40}$$

The first term on the right-hand side in Eq. (39) represents losses of the Stokes wave and lowers the threshold (due to the exponentially decreasing function), as the order of the resonance increases and the losses decrease. The second term on the right-hand side of Eq. (39) represents resonance of the laser wave, and it is also expected to reduce the threshold. Let us compare now the threshold intensity obtained for a sphere with that obtained for a linear cavity. For a linear cavity we may take the threshold condition to be given by

$$E_0^2 \geqslant \frac{\Gamma_s}{\alpha_{s,l}}, \tag{41}$$

where Γ_s are the Stokes wave losses and $\alpha_{s,l}$ is the gain constant. Neglecting absorption and diffraction losses and taking into account only cavity end losses we have

$$\Gamma_s = \frac{cT}{mL}. \tag{42}$$

Here c, T, m, and L, are the speed of light, transmittance of the mirrors, the index of refraction, and the cavity length, respectively. Comparison between the last expression and Eq. (41) shows that we indeed get a *drastic reduction* of threshold condition, due to the presence of exponentially decreasing factor. A more careful inspection of Eq. (41) shows that, in fact, threshold intensity is an oscillating function of the size parameter, due to the spherical Bessel function in the denominator of Eq. (41). This behavior is a consequence of the resonant nature of the sphere. Linewidth would become broadened on increasing the size parameter and thus the threshold intensity would increase as a function of size parameter. The most interesting physical behavior is that the energy losses of high order modes in microspheres become smaller, in contrast with what happens in a linear cavity in which losses increase for high order modes. Figure 4 shows the threshold intensity in the microsphere compared to the linear cavity case, where we have fixed the Stokes parameters to correspond to $TE_{90,1}$ resonance and varied the laser size parameter (wavelength). We take the Stokes size parameter to be $\rho_{0,s}=72.261$, which corresponds to a wavelength of $\lambda_s=525$ nm for a 6.12 μm droplet (radius). The index of refraction is $m=1.33$ (water). For the linear cavity we have chosen $L=0.1$ m, $T=0.01$. We can see that there exists a drastic reduction of threshold intensity, of about ten orders of magnitude, near the point $\rho=74.2$. Note the different scales of the two graphs. For lower order modes that are more lossy, the reduction of threshold intensity can be less pronounced and even worse than that of the linear cavity, but the main point is that the microsphere, being a selective system, will favor higher modes that are less lossy.

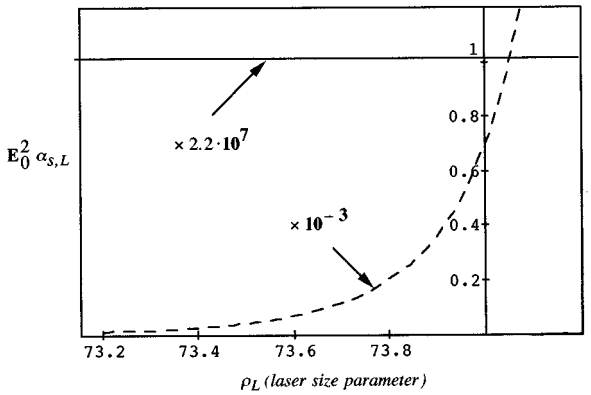

FIG. 4. Comparison of threshold intensity, as a function of size parameter, between linear cavity (solid line) and the sphere. The Stokes wave parameters were chosen to coincide with $TE_{90,1}$ resonance, with size parameter $\rho_s=73.261$, for a 6.1 μm water droplet ($m=1.33$). $L=0.1$ m, $T=0.01$. Note the different scales here.

IV. CONCLUSION

We have constructed an approximate analytic approach which allows an adequate assessment of a threshold for nonlinear interaction in microspheres. Systematic investigation of the characteristic equation, using approximate analytic expressions, reveals that not all modes have the same quality. In particular, modes characterized by external wave ''obeying'' the ''no oscillation'' approximation, and internal waves for which their argument corresponds to the stationary phase approximation, are characterized by very high quality, and correspond to a physical situation in which the spherical wave can be envisioned as whispering-gallery light waves that are totally internally reflected by the sphere boundary, without suffering almost any loss. We have derived an approximate characteristic equation, transcendental in fact, but which is very simple. It predicts correct resonance positions and can be used as a very good alternative to the exact characteristic equation. The resonance width was found to be an exponentially decreasing function of the mode number (angular momentum). Threshold intensity evaluation in the most interesting cases, of very high mode quality, has shown a dramatic reduction, with respect to the same process in a conventional linear cavity. Though our theory was exemplified in the case of stimulated Raman scattering, it can easily be applied to other nonlinear and quantum optics processes.

[1] J. Z. Zhang, D. H. Leach, and R. K. Chang, Opt. Lett. **13**, 270 (1988).

[2] V. B. Braginsky, M. L. Grodetsky, and V. S. Ilchenk, Phys. Lett. A **137**, 393 (1989).

[3] P. W. Barber, *Light Scattering by Particles* (World Scientific, Singapore, 1990); D. S. Benincasa *et al.*, Appl. Opt. **26**, 1348 (1987); G. J. Rosasco and H. S. Bennett, J. Opt. Soc. Am. **68**, 1242 (1978).

[4] P. Goy, J. M. Raimond, M. Gross, and S. Haroche, Phys. Rev. Lett. **50**, 1903 (1983); D. Klepner, *ibid.* **55**, 2137 (1985).

[5] R. E. Benner, P. W. Barber, J. F. Owen, and R. K. Chang, Phys. Rev. Lett. **44**, 475 (1980).

[6] H. B. Lin, J. D. Eversole, C. D. Merrit, and A. J. Campillo, Phys. Rev. A **45**, 6756 (1992).

[7] A. J. Campillo, J. D. Eversole, and H-B. Lin, Phys. Rev. Lett. **67**, 437 (1991).

[8] H-B. Lin, J. D. Eversole, and A. J. Campillo, Opt. Lett. **17**, 828 (1992).

[9] H-B. Lin and A.J. Campillo, Phys. Rev. Lett. **73**, 2240 (1994).

[10] S. C. Hill, D. H. Leach, and R. K. Chang, J. Opt. Soc. Am. B **10**, 16 (1993).

[11] S. M. Chitanvis and C. D. Cantrell, J. Opt. Soc. Am. B **6**, 1326 (1989).

[12] P. T. Leung and K. Young, Phys. Rev. A **44**, 593 (1991).

[13] C. C. Lam, P. T. Leung, and K. Young, J. Opt. Soc. Am. B **9**, 1585 (1992).

[14] J. A. Stratton, *Electromagnetic Theory* (McGraw-Hill, New York, 1941).

[15] I. S. Gradshteyn and I. M. Ryzhik, *Table of Integrals, Series and Products* (Academic Press, New York, 1965).

[16] K. Hayata and M. Koshiba, Phys. Rev. A **46**, 6104 (1992); J. Cooney and A. Gross, Opt. Lett. **7**, 218 (1985); J. B. Snow, S. X. Qian, and R. K. Chang, *ibid.* **10**, 39 (1985); H.-M. Tzeng *et al.*, *ibid.* **9**, 499 (1984); H. Chew, D.-S. Wang, and M. Kerker, J. Opt. Soc. Am. B **1**, 56 (1984); G. Kurizki and A. Nitzan, Phys. Rev. A **38**, 267 (1988).

[17] G. N. Watson, *A Treatise on the Theory of Bessel Functions*, 2nd ed. (Cambridge University Press, Cambridge, 1958), pp. 135 and 136.